DYNAMIC STRUCTURAL MODEL OF A SUBMERGED RING

Jack Thomas Waller

NAVAL POSTGRADUATE SCHOOL
Monterey, California

THESIS

DYNAMIC STRUCTURAL MODEL
OF A SUBMERGED RING

by

Jack Thomas Waller Jr.

September 1979

Thesis Advisor: R. E. Newton

REPORT DOCUMENTATION PAGE		READ INSTRUCTIONS BEFORE COMPLETING FORM
1. REPORT NUMBER	2. GOVT ACCESSION NO.	3. RECIPIENT'S CATALOG NUMBER
4. TITLE (and Subtitle) Dynamic Structural Model of a Submerged Ring		5. TYPE OF REPORT & PERIOD COVERED Master's Thesis; September 1979
		6. PERFORMING ORG. REPORT NUMBER
7. AUTHOR(s) Jack Thomas Waller Jr.		8. CONTRACT OR GRANT NUMBER(s)
9. PERFORMING ORGANIZATION NAME AND ADDRESS Naval Postgraduate School Monterey, California 93940		10. PROGRAM ELEMENT, PROJECT, TASK AREA & WORK UNIT NUMBERS
11. CONTROLLING OFFICE NAME AND ADDRESS Naval Postgraduate School Monterey, California 93940		12. REPORT DATE September 1979
		13. NUMBER OF PAGES 50
14. MONITORING AGENCY NAME & ADDRESS(if different from Controlling Office)		15. SECURITY CLASS. (of this report) Unclassified
		15a. DECLASSIFICATION/DOWNGRADING SCHEDULE

16. DISTRIBUTION STATEMENT (of this Report)

Approved for public release; distribution unlimited.

17. DISTRIBUTION STATEMENT (of the abstract entered in Block 20, if different from Report)

18. SUPPLEMENTARY NOTES

19. KEY WORDS (Continue on reverse side if necessary and identify by block number)

Structural Ring
Trigonometric Series
Underwater Shock
Fluid Structure Interface

20. ABSTRACT (Continue on reverse side if necessary and identify by block number)

A dynamic structural model of a submerged ring is developed using trigonometric series. It is constructed for use in conjunction with a finite element fluid model to examine the effects of cavitation on underwater shock loading of a structure. The governing equations and the time integration algorithm used in the model are described.

(20. ABSTRACT Continued)

Results predicted by the model are compared to known results. The program listing is given.

Dynamic Structural Model of a Submerged Ring

by

Jack Thomas Waller Jr.
B.S.M.E., New Mexico State University, 1975

Submitted in partial fulfillment of the requirements for the degree of

MASTER OF SCIENCE IN MECHANICAL ENGINEERING

from the

NAVAL POSTGRADUATE SCHOOL
September 1979

ABSTRACT

A dynamic structural model of a submerged ring is developed using trigonometric series. It is constructed for use in conjunction with a finite element fluid model to examine the effects of cavitation on underwater shock loading of a structure. The governing equations and the time integration algorithm used in the model are described. Results predicted by the model are compared to known results. The program listing is given.

TABLE OF CONTENTS

LIST OF TABLES

LIST OF FIGURES

LIST OF SYMBOLS

A	-	cross sectional area of the ring (m^2)
a_n	-	Fourier cosine coefficient for radial displacement (m)
b_n	-	Fourier sine coefficient for tangential displacement (m)
c	-	speed of sound in ring material (m/s)
c_n	-	Fourier cosine coefficient for normal pressure (Pa)
D	-	flexural rigidity of the ring ($N \cdot m^2$)
E	-	modulus of elasticity of the ring material (Pa)
h	-	time step used in central difference integration (sec)
I	-	area moment of inertia about centroidal axis (m^4)
κ	-	curvature of the ring (1/m)
M	-	bending moment about centroidal axis ($N \cdot m$)
ω_n	-	natural circular frequency of vibration (rad/s)
r	-	centroidal radius of gyration of ring cross section (m)
R	-	radius of ring (m)
ρ	-	density of ring material (kg/m^3)
θ	-	angle between normal to shock plane and location on the ring (radians)
v	-	tangential displacement (m)
w	-	radial displacement (m)
z	-	$(r/R)^2$

ACKNOWLEDGEMENT

The author wishes to express his sincere appreciation to Dr. Robert E. Newton, Professor of Mechanical Engineering, for his patience and guidance which made this investigation possible. Also, the author thanks his wife, Belen, for her support throughout his work.

I. INTRODUCTION

The program evolved during this study models a submerged circular ring using trigonometric series. It was developed for use in conjunction with a finite element fluid model based on a displacement potential formulation. The purpose of the combined models is to predict the effects of cavitation on underwater shock loading of the structure. More information on the fluid model can be found in References 1 and 2. The purpose of this paper is to describe the development of the structural model and to present some of the results obtained from its use in combination with the fluid model. A listing of the FORTRAN IV program implementing the structural model is given in the Appendix.

II. GOVERNING EQUATIONS

A. DIFFERENTIAL EQUATIONS FOR THE DEFLECTION OF A THIN CIRCULAR RING

In Figure 1 the solid line represents the ring after deformation, and the dotted line the ring before deformation. For small deflections the curvature of the element $m_1 n_1$ can be taken as

$$\frac{1}{R_1} = \frac{d\theta + \Delta d\theta}{ds + \Delta ds}$$

where R, w, θ and s are defined as shown in Figure 1 and w is taken positive inward. Making use of the relations

$$\Delta d\theta = d\theta_1 - d\theta = \frac{dw}{ds} + \frac{d^2w}{ds^2} ds - \frac{dw}{ds} = \frac{d^2w}{ds^2} ds$$

$$\Delta ds = ds_1 - ds = (r - w) d\theta - r d\theta = -w d\theta = -w \frac{ds}{R}$$

and substituting into the equation above yields

$$\frac{1}{R_1} = \frac{d\theta + \frac{d^2w}{ds^2} ds}{ds(1 - \frac{w}{R})} = \frac{d\theta(1 + \frac{w}{R})}{ds(1 - \frac{w}{R})(1 + \frac{w}{R})} + \frac{\frac{d^2w}{ds^2} ds(1 + \frac{w}{R})}{ds(1 - \frac{w}{R})(1 + \frac{w}{R})}$$

Neglecting the higher order terms, the above expression becomes

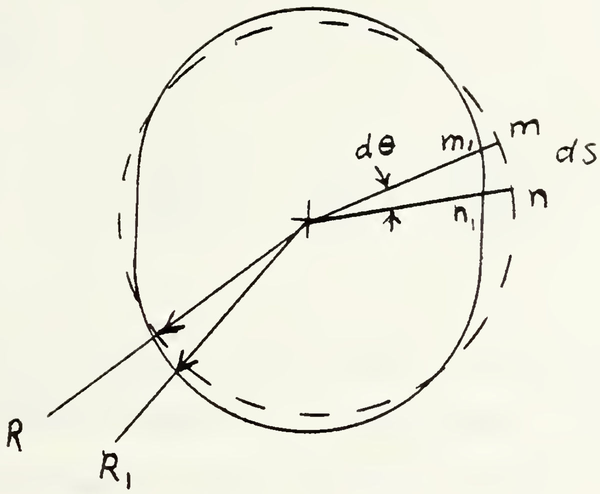

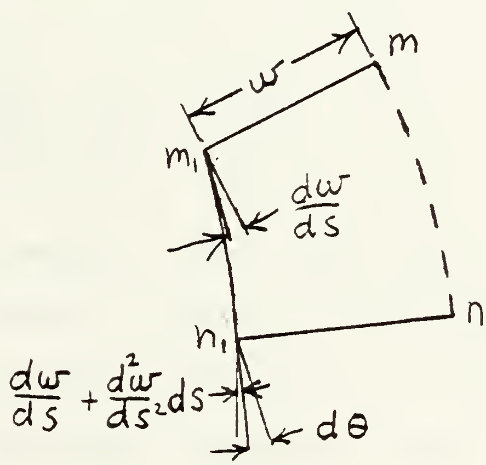

Figure 1. Geometry of Ring Deformation

$$\frac{1}{R_1} = \frac{d\theta}{ds}\left(1 + \frac{w}{R}\right) + \frac{d^2w}{ds^2} = \frac{1}{R}\left(1 + \frac{w}{R}\right) + \frac{d^2w}{ds^2}$$

or alternately

$$\frac{1}{R_1} - \frac{1}{R} = \frac{w}{R^2} + \frac{d^2w}{ds^2} = \frac{1}{R^2}\left(w + \frac{d^2w}{d\theta^2}\right) \qquad (1)$$

For a ring where the thickness is small compared to the radius and elastic behavior is assumed, it can be shown that the approximate relationship between deflection and loading is [Reference 7]

$$\frac{1}{R_1} - \frac{1}{R} = -\frac{M}{D} \qquad (2)$$

where M is the bending moment about the centroidal axis and D is the flexural rigidity of the ring. A positive bending moment produces compression in the outside fibers of the ring. Combining equations 1 and 2 yields the differential equations for the deflection of the ring given below.

$$\frac{1}{R^2}\left(\frac{\partial^2 w}{\partial\theta^2} + w\right) = -\frac{M}{D} \qquad (3)$$

B. GOVERNING EQUATIONS OF MOTION

The governing equations of motion used in the program were arrived at by the application of Hamilton's principle. In order to apply Hamilton's principle, it is first necessary to derive expressions for the strain energy and kinetic energy of the ring as well as the work done by the external loads. In these derivations the ring was taken to be homogeneous, elastic, and of unit width. The pressures on the ring and its deflection were represented by the pressures at and the deflection of a set of nodal points equally spaced along the circumference of the ring.

The shock front is assumed to approach the ring normal to the $\theta = 0$ plane as shown in Figure 2, where θ is taken to be positive counterclockwise.

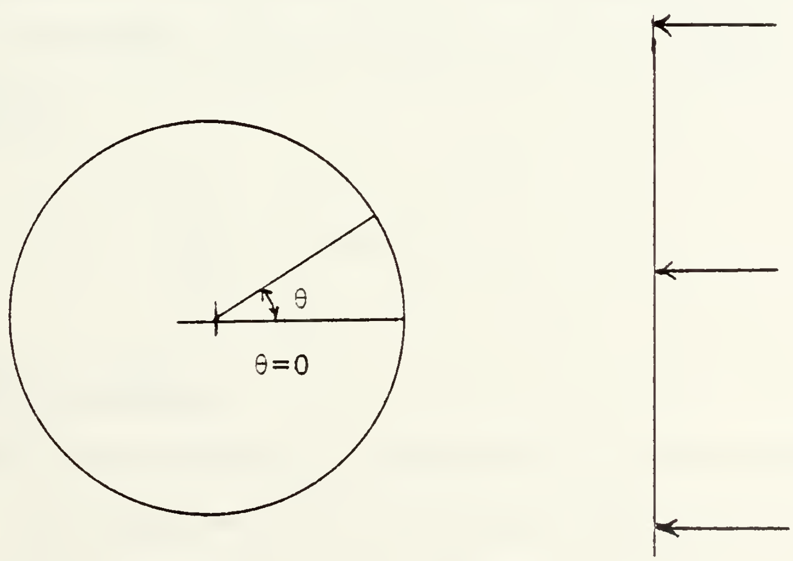

Figure 2. Ring, Shock Front Orientation

Since the ring is symmetric about the $\theta = 0$ plane, results are given for θ from 0° to 180°. The response of the ring is represented by the response of a set of N+1 nodal points equally spaced along the ring. The radial displacement is approximated by a trigonometric cosine series

$$w = \sum_{n=0}^{N} a_n \cos n\theta \quad . \tag{4}$$

The tangential deflection is represented by the trigonometric sine series

$$v = \sum_{n=1}^{N} b_n \sin n\theta \quad , \tag{5}$$

where v is taken to be positive in the negative θ direction. Similarly the normal pressure applied to the ring is represented by

$$p = \sum_{n=0}^{N} c_n \cos n\theta \quad . \tag{6}$$

1. Strain Energy

The strain energy is comprised of two components [Ref. 4]. One component is the strain energy due to bending and the other to strain in the θ direction (ε_θ). The strain energy stored in the ring due to bending is calculated as

the work done by the internal moment acting over the entire ring, and for a ring of unit width is

$$U_B = \frac{1}{2} \int_0^{2\pi} M\ R\kappa d\theta$$

where κ is the curvature of the ring. Combining this equation with equation 3 and using the relation $\kappa = M/D$ yields

$$U_B = \frac{1}{2} \int_0^{2\pi} D \frac{1}{R^3} \left(\frac{\partial^2 w}{\partial \theta^2} + w\right)^2 d\theta \qquad (7)$$

The strain energy due to the strain in the θ direction is obtained as the distance traveled by the average normal force in the θ direction.

The circumferential strain is composed of two components the first of which is the result of the radial displacement of the ring $(\frac{w}{R})$ and the second results from tangential displacement and is $(\frac{1}{R} \frac{\partial v}{\partial \theta})$. The strain energy from the normal force (N) is

$$U_\theta = \frac{1}{2} \int_0^{2\pi} N\varepsilon_\theta R\ d\theta = \frac{1}{2} \int_0^{2\pi} A\varepsilon_\theta E\varepsilon_\theta R\ d\theta$$

or (8)

$$U_\theta = \frac{1}{2} \int_0^{2\pi} RAE{\varepsilon_\theta}^2\ d\theta = \frac{1}{2} \int_0^{2\pi} \frac{AE}{R^2} \left(\frac{\partial v}{\partial \theta} + w\right)^2 Rd\theta$$

where A is the cross sectional area of the ring and

E is the modulus of elasticity of the ring material.

Combining equations 7 and 8, the expression for the total strain energy is

$$U_T = \frac{1}{2}\int_0^{2\pi} \frac{D}{R^3}\left(\frac{\partial^2 w}{\partial \theta^2} + w\right)^2 d\theta + \frac{1}{2}\int_0^{2\pi} \frac{AE}{R}\left(\frac{\partial v}{\partial \theta} + w\right)^2 d\theta \qquad (9)$$

Substituting into this equation the series expressions for radial and tangential displacements, and assuming constant geometrical and material properties over the ring yields after integration

$$U_T = \frac{\pi D}{2R^3}\left[\sum_{n=0}^{N} a_n^2 (n^2-1)^2 + \frac{AE\pi}{2R}\left[\sum_{n=0}^{N} (nb_n + a_n)^2\right]\right. \quad *$$

An expression for the change in strain energy δU corresponding to small changes in tangential and radial displacements (δb_n and δa_n) can now be found

$$\delta U = \frac{\pi D}{3}\left[\sum_{n=0}^{N} (n^2-1)^2 a_n \delta a_n\right] + \frac{AE\pi}{R}\left[\sum_{n=0}^{N} (n^2 b_n + na_n)\delta b_n + (nb_n + a_n)\delta a_n)\right] \qquad (10)$$

---

*In this equation and several that follow which contain a summation expression starting with n = 0, a factor of 2 associated with the n = 0 term is omitted for the sake of brevity. The term is accounted for in the solution process used with the model.

2. Work

The work associated with a small change in radial displacement is given by

$$\delta W = \int_0^{2\pi} p \; \delta w \; R \; d\theta$$

Substituting the relations

$$p = \sum_{m=0}^{N} c_m \cos m\theta$$

and

$$\delta w = \sum_{n=0}^{N} \delta a_n \cos n\theta$$

into this expression yields, after integration

$$\delta W = \sum_{n=0}^{N} c_n \; \delta a_n \; \pi R$$

3. Kinetic Energy

The expression for the kinetic energy of the ring can be arrived at by considering an infinitesimal section of the ring that has been set in motion. The kinetic energy of the element can be represented as the sum of a contribution due to translation of the mass center and a contribution due to rotation. This leads to

$$dT = \frac{1}{2}\rho(ARd\theta)(\dot{w}^2 + \dot{v}^2) + \frac{1}{2}\rho IRd\theta\left(\frac{\partial \dot{w}}{R\partial\theta}\right)^2$$

where I is the area moment of inertia about the centroidal axis.

Using the series relations

$$w = \sum_{n=0}^{N} a_n \cos n\theta \qquad \dot{w} = \sum_{n=0}^{N} \dot{a}_n \cos n\theta$$

$$v = \sum_{n=1}^{N} b_n \sin n\theta \qquad \dot{v} = \sum_{n=1}^{N} \dot{b}_n \sin n\theta$$

yields

$$dT = \frac{1}{2}\rho(ARd\theta)\left[\left(\sum_{n=0}^{N} \dot{a}_n \cos n\theta\right)^2 + \left(\sum_{n=1}^{N} \dot{b}_n \sin n\theta\right)^2\right]$$

$$+ \frac{1}{2}\rho IRd\theta\left(- \frac{1}{R}\sum_{n=1}^{N} \dot{a}_n\, n \sin n\theta\right)^2$$

Integration over the ring yields

$$T = \frac{\pi\rho}{2} \sum_{n=0}^{N} \left[\left(AR + n^2 \frac{I}{R}\right)\dot{a}_n^{\,2} + AR\dot{b}_n^{\,2}\right]$$

The resultant change in kinetic energy due to a small change in velocity components can then be found as

$$\delta T = \pi\rho \sum_{n=0}^{N} \left[\left(AR + n^2 \frac{I}{R}\right)\dot{a}_n \delta\dot{a}_n + AR\dot{b}_n \delta\dot{b}_n\right] \qquad (12)$$

4. Application of Hamilton's Principle To Find Coupled Equations of Motion

From Hamilton's principle [Ref. 5] it is known that

$$\int_{t_1}^{t_2} (\delta T - \delta U + \delta W)\, dt = 0 \qquad (13)$$

Combining equations 10, 11, 12 and 13 yields, after carrying out an integration by parts on the first term,

$$\sum_{n=0}^{N} \pi\rho(AR + n^2 \tfrac{I}{R})[\dot{a}_n \delta a_n \Big|_{t_1}^{t_2} - \int_{t_1}^{t_2} \ddot{a}_n\, \delta a_n\, dt]$$

$$+ \sum_{n=0}^{N} \pi\rho AR[\dot{b}_n\, \delta b_n \Big|_{t_1}^{t_2} - \int_{t_1}^{t_2} \ddot{b}_n\, \delta b_n\, dt]$$

$$- \int_{t_1}^{t_2} \{\frac{\pi D}{R^3} [\sum_{n=0}^{N} (n^2-1)^2\, a_n\, \delta a_n] + \frac{AE\pi}{R} [\sum_{n=0}^{N} (n^2 b_n + na_n)\delta b_n$$

$$+ (nb_n + a_n)\delta a_n] - \sum_{n=0}^{N} c_n\, \delta a_n\, \pi R\}\ dt = 0$$

Since the δa_n and δb_n can be chosen arbitrarily, this becomes

$$(1 + (\tfrac{r}{R})^2\, n^2)\ddot{a}_n + (\tfrac{c}{R})^2[1 + (\tfrac{r}{R})^2(n^2 - 1)^2]a_n + (\tfrac{c}{R})^2 = \frac{c_n}{\rho A}$$

$$\ddot{b}_n + (\tfrac{c}{R})^2\, na_n + (\tfrac{c}{R})^2\, n^2 b_n = 0 \qquad (14)$$

where $c = (E/\rho)^{1/2}$ is the speed of sound in the ring and

where r is the centroidal radius of gyration of the ring section and the relation $I = Ar^2$ has been used.

5. Separated Equations of Motion

It is common practice to separate ring deformations into flexural modes and extensional modes. The initial version of this program utilized such a resolution. The flexural mode is characterized by the requirement that

$$\varepsilon_\theta = -(w + \frac{\partial v}{\partial \theta})/R = 0 \ .$$

This implies that the Fourier coefficients satisfy the relation

$$a_{n(F)} + nb_{n(F)} = 0 \qquad (15)$$

The extensional mode is defined to be geometrically orthogonal to the flexural mode so that

$$na_{n(E)} - b_{n(E)} = 0 \qquad (16)$$

Substituting equation 15 into equations 14 yields the result

$$[\rho A((\frac{n^2+1}{n^2}) + zn^2)]\ddot{a}_{n(F)} + [\frac{EA}{R^2} z(n^2-1)^2]\ a_{n(F)} = c_n$$

$$b_{n(F)} = -a_{n(F)}/n \qquad (17)$$

where $z = (r/R)^2$.

If equation 16 is substituted into equations 14, the result is

$$[\rho A((n^2+1) + zn^2)]\ddot{a}_{n(E)} + [\frac{EA}{R^2}((n^2+1)^2 + z(n^2-1)^2]a_{n(E)} = c_n \qquad (18)$$

$$b_{n(E)} = na_{n(E)}$$

Initial solutions were carried out using equations 17 and 18 and then combining the results by

$$a_n = a_{n(F)} + a_{n(E)}$$

$$b_n = b_{n(F)} + b_{n(E)}$$

This procedure gave results which satisfactorily predicted the ring bending moments but gave poor accuracy for axial force determinations.

Re-examination of the foregoing solution process revealed that the mode shapes defined by equations 15 and 16 are not orthogonal with respect to the mass or the stiffness matrices of the system. It was accordingly decided to return to equations 14 and solve them

simultaneously in the time integration algorithm. This change led to accurate axial force determinations. The separated equations of motion, 17 and 18, are used in the program as described in Section III, b.

III. TIME INTEGRATION METHOD

A. CENTRAL DIFFERENCE ALGORITHM

Time integration is accomplished using a central difference algorithm. If a_n, b_n, and c_n are known at time $t^{(i)}$, then $\ddot{a}_n^{(i)}$ (the value of $\ddot{a}_n$ at $t^{(i)}$) may be evaluated from the first of equations 14. Letting h represent the time step and $\dot{a}_n^{(i-\frac{1}{2})}$ represent $\dot{a}_n$ at time $t^{(i)} - h/2$, the next value of $\dot{a}_n$ is calculated from

$$\dot{a}_n^{(i+\frac{1}{2})} = \dot{a}_n^{(i-\frac{1}{2})} + h\ddot{a}_n^{(i)} \tag{19}$$

Using this result, the next a_n (at time $t^{(i+1)} = t^{(i)} + h$) is calculated from

$$a_n^{(i+1)} = a_n^{(i)} + h\,\dot{a}_n^{(i+\frac{1}{2})} \tag{20}$$

The value $\ddot{b}_n^{(i)}$ is similarly found from the second of equations 14. A pair of equations paralleling 19 and 20 are used to calculate $\dot{b}_n^{(i+\frac{1}{2})}$ and $b_n^{(i)}$. When these steps have been completed for each n, the value of radial displacement w is found at each structural node from equation 4. These displacements are passed to the fluid program where they furnish required interface boundary conditions to allow an advance to time $t^{(i+1)}$. Values of fluid pressure at the interface nodes are returned by the fluid program.

The new nodal pressures are used to calculate c_n's at $t^{(i+1)}$. It is then again possible to advance $\dot{a}_n$ and a_n using equations 14, 19, and 20 and to perform the parallel calculations for $\dot{b}_n$ and b_n.

The solution process is started with the ring at rest under uniform hydrostatic pressure. Under the loading a_0 is the only nonzero Fourier coefficient. Because $\dot{a}_n^{(0)} = 0$ is known (rather than $\dot{a}_n^{(-\frac{1}{2})}$, a fictitious starting value of $\dot{a}_n^{(-\frac{1}{2})}$ is first calculated from

$$\dot{a}_n^{(-\frac{1}{2})} = -\frac{h}{2}\ddot{a}_n^{(0)}$$

A similar starting procedure is used for $\dot{b}_n$.

B. SELECTION OF THE NUMBER OF VIBRATIONAL MODES USED

The number of vibrational modes that can be modeled accurately is limited by the numerical integration algorithm. Specifically, the algorithm becomes unstable for time steps in excess of about 0.3 of the period of the structural mode. The accuracy of the algorithm deteriorates even before the stability limit is reached. For this reason, a criterion was established for limiting the number of modes used, based on the time steps selected.

In the program the separated equations of motion for the extensional and flexural modes were used to find the frequencies needed in applying the criterion. From

equations 17 and 18 the natural frequencies of the extensional and flexural modes were found to be

$$\omega_{n(E)}^2 = \left(\frac{c}{R}\right)^2 (1 + n^2) \qquad n = 0,1,2,3,...$$

$$\omega_{n(F)}^2 = \left(\frac{c}{R}\right)^2 \left(\frac{r}{R}\right)^2 \frac{n^2(n^2 - 1)^2}{n^2 + 1} \qquad n = 2,3,4,...$$

The criterion used was that the period for the highest mode retained be at least five times the time step used. Since the extensional modes have higher frequencies for a given n, this criterion comes into effect first for the extensional modes. Once the point is reached (where $n = n_E(\max)$), the program switches from the coupled equations of motion 14, to the separated equation 17. When this occurs the higher extensional mode coefficients ($n > n_E(\max)$) are not needed, and only the flexural mode coefficients (for $n > n_E(\max)$) are used. If the time step is large enough that the criterion is also met by the flexural modes ($n = n_F(\max)$) then both the a_n's and b_n's are omitted for all modes where n is greater than $n_F(\max)$.

IV. RESULTS

To check the accuracy of the results obtained from the program, two kinds of comparisons were made. First, the solution of equations 14 arrived at by the program were compared to an analytic solution of equations 14. Second, to verify that equations 14 correctly predict ring behavior, calculated dynamic response of the ring to two particular loadings was compared to known static results [Reference 6] for the same loadings.

A. COMPARISON OF MODEL RESULTS TO EXACT SOLUTION

The check on solution accuracy was based on the exact solution for a ring initially at rest and suddenly loaded by a steady pressure

$$P = [1.625 - .25 \cos \theta - .375 \cos 2\theta] \text{ MPa}$$

The exact solution, using the parameters specified in Table I, is

$$\begin{aligned} a_0 &= 4.05844\text{x}10^{-3}[1 - \cos (1011.303t)] \\ a_1 &= -159.483t^2 - 1.5617\text{x}10^{-4}[1 - \cos (1429.t)] \\ a_2 &= -.104129[1 - \cos (85.616)t] \\ &\quad - 3.7355\text{x}10^{-5}[1 - \cos (2259.7t)] \end{aligned} \tag{22}$$

Table I gives results for radial displacements at $t = 1$ msec for $\theta = 0°$, $90°$ and $180°$. Computer results are given for four different time steps. Even the coarsest time step gives results within 1% of the exact values obtained from equations 22.

B. COMPARISON OF MODEL RESULTS TO STATIC BEHAVIOR

To compare the dynamic response predicted by the program to the known static response of the ring for the same loading, two simple cases of loading were assumed. The first loading case examined was uniform pressure surrounding the ring; the second case was two equal and opposite concentrated loads acting 180° apart as shown in Figure 3. The second loading case could not be represented exactly by the finite trigonometric series loading representation used by the program. It was approximated by nonzero values of pressure only at $\theta = 0°$ and $\theta = 180°$.

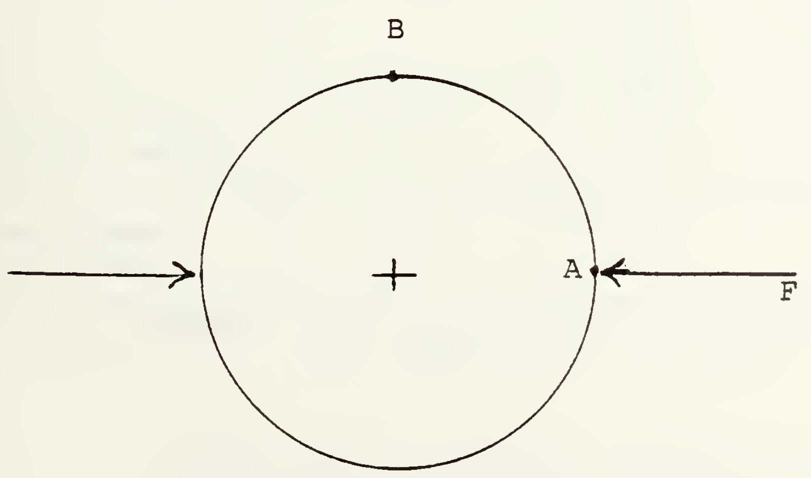

Figure 3. Concentrated Loading on Ring

TABLE I

	Time Step sec	ΔR NP1 $m \times 10^{-7}$	ΔR NP2 $m \times 10^{-7}$	ΔR NP3 $m \times 10^{-7}$
ΔR predicted by program	2.5×10^{-4}	11619.	23687.	17556.
	1×10^{-5}	11679	23472.	17553
	1×10^{-6}	11682	23469.	17555.
	1×10^{-7}	11683.	23469.	17555.
ΔR from equations 17		11683.	23469.	17555.

Ring Parameters: $R = 5$ m, $A = .05$ m^2, $E = 200$ GPa
$\rho = 7830$ kg/m^3, $r = .158$m

Comparison of program solution with analytic solution

TABLE II

	ΔR (max) mm	Axial Force (Max) MN
Program results	4.98	-9.8
Twice Known Static Results	5.00	-10.0

Ring Parameters: $R = 5$ m, $A = .05$ m^2, $E = 200$ GPa
$\rho = 7830$ kg/m^3, $r = .158$ m

Comparison of program dynamic solution with twice known static solution for uniform external pressure on ring

Comparison between the dynamic and static responses of the ring were made for the radial displacements, bending moments, and forces at particular nodal points on the ring. For the uniform pressure case any nodal point on the ring can be used since the displacements are uniform over the ring. For the concentrated loading case, the nodal points chosen were at the points of application of the forces and midway between the application points.

For the dynamic response of the ring predicted by the program, the ring is taken to be initially at rest and undeformed. The anticipated behavior of the ring after the application of the loading is for the ring to deflect through the radial displacements found for the static loading and to continue to deflect until a radial displacement with a magnitude of approximately twice the static displacement is reached. The maximum deflections were expected to occur after a time approximately equal to one half the period of the vibrational mode that dominates the deflection of the ring. For the uniform loading case the dominant vibrational mode is the fundamental extensional mode. For the concentrated loading case, it is the second flexural mode. The periods for these vibrational modes can be found using equations 21. Tables II and III give the comparisons between the dynamic response from the program and twice the known static response for the two loading cases considered. As is seen, relatively good correlations

TABLE III

Number of Nodal Points Used		ΔR_A (max) m	ΔR_B (max) m	Axial Force at B MN	Bending Moment at B MN·m
5	Model Results	.2965	-.2839	-3.760	-7.910
	Static Analysis Results Times 2	.2634	-.2421	-3.536	-6.434
7	Model Results	.2013	-.1857	-2.353	-4.737
	Static Analysis Results Times 2	.1862	-.1713	-2.500	-4.543
9	Model Results	.1510	-.1393	-1.743	-3.544
	Static Analysis Results Times 2	.1425	-.1311	-1.913	-3.477

Ring Parameters: $R = 5$ m, $A = .05$ m^2, $E = 200$ GPa
$\rho = 7830$ kg/m^3, $r = .158$ m

Comparison of dynamic solution with twice known static solution for loading of Fig. 3

between the dynamic responses and twice the static responses were obtained. The maximum values shown in Table III occur at approximately 35.3 milliseconds after time zero, which compares favorably to one half of the period of the second flexural mode (36.6 milliseconds). The maximum values in Table II occur at 3 milliseconds which is approximately one half the period of the fundamental extensional mode (3.11 milliseconds).

C. OUTPUT EXAMPLES

A sample of the output produced by the structural program is shown in Figures 4 and 5. The print code at the top of Figure 4 is an input code used to select the information desired in the print out. Following the print code are two sets of input parameters to be used in the structural model. These are followed by the mass and stiffness coefficients calculated for each of the vibrational modes. This information remains constant for any given run and is therefore only printed once. The rest of the information varies with time and can be printed as often as desired. The pressures at nodal points generated by the fluid model are printed out; these pressures are for one time step before the time printed below the pressures. Following the time come the Fourier coefficients for the radial displacements, tangential displacements, and pressures. In Figure 5 at the top, the bending moment and the axial force

at each nodal point are printed for the time given in Figure 4. Tabulation of the radial displacement follows.

Figure 6 is an example of the graphical output obtained from the fluid model when the fluid and structural models are run jointly. It is a time sequence of eight plots of fluid nodal pressures over the domain. The plots are shown at 8 ms intervals. The left hand edge of each plot represents the plane of symmetry and the top and bottom rows represent, respectively, the entry and exit faces for the shock. The x's on the lower left side of the plots represent dummy nodes inside the structure. The pressure ranges for the mapping characters are shown in Figure 7. In Figure 6 the development of the cavity can be followed. It develops in the second, third, and fourth frames, collapses in the fifth, and has vanished by the sixth.

PRINT CODE: 121111111 1 112 11415161718 1 1

NNEL	NNP	M	N	NNPA1N	NNPA2N
16	17	2	0	9	17

A	E	P	RI	RHO
0.500D-01	0.200D 12	5.00	0.158	0.783D 04

I	XKA1N	XKA2N	XMA1N	XKB1N
1	0.40040D 09	0.0	391.50	0.0
2	0.40000D 09	0.10217D 07	391.89	0.40000D 09
3	0.40360D 09	0.20434D 07	393.07	0.80000D 09
4	0.42560D 09	0.30651D 07	395.02	0.12000D 10
5	0.49000D 09	0.40868D 07	397.76	0.16000D 10
6	0.63040D 09	0.51086D 07	401.29	0.20000D 10
7	0.89000D 09	0.61303D 07	405.59	0.24000D 10
8	0.13216D 10	0.71520D 07	410.68	0.28000D 10
9	0.19876D 10	0.81737D 07	416.56	0.32000D 10
10	0.29600D 10	0.91954D 07	423.21	0.36000D 10
11	0.43204D 10	0.10217D 08	430.65	0.40000D 10
12	0.61600D 10	0.11239D 08	438.87	0.44000D 10
13	0.85796D 10	0.12261D 08	447.88	0.48000D 10
14	0.11690D 11	0.13282D 08	457.66	0.52000D 10
15	0.15610D 11	0.14304D 08	468.23	0.56000D 10
16	0.20470D 11	0.15326D 08	479.59	0.60000D 10
17	0.26410D 11	0.16347D 08	491.72	0.64000D 10

NODAL POINT PRESSURES

0.12D 08	0.98D 07	0.56D 07	0.21D 07	0.52D 06	0.23D 06
0.21D 06	0.20D 06	0.20D 06	0.20D 06	0.21D 06	0.21D 06
0.16D 06	0.20D 06	0.20D 06	0.20D 06	0.20D 06	

TIME = 0.250 MS

BN	AN	CN
0.0	0.59923D-03	0.16297D 07
-0.43636D-05	0.19121D-03	0.27357D 07
-0.76030D-05	0.16725D-03	0.23797D 07
-0.90952D-05	0.13425D-03	0.18891D 07
-0.87862D-05	0.98196D-04	0.13588D 07
-0.70538D-05	0.63918D-04	0.86420D 06
-0.48681D-05	0.37398D-04	0.48802D 06
-0.27813D-05	0.18732D-04	0.23172D 06
-0.11520D-05	0.65591D-05	76529.
-0.24765D-06	0.22299D-05	18334.
0.76762D-08	-0.76762D-07	-8451.9
0.70517D-07	-0.77569D-06	-15526.
0.11450D-07	-0.13740D-05	-4825.4
0.64630D-07	-0.84018D-06	-14242.
0.48881D-07	-0.68433D-06	-10768.
0.38325D-07	-0.57487D-06	-8187.1
0.33831D-07	-0.54130D-06	-9139.7

Fig. 4. Output Example

NP	MOMENT	FORCE
1	61466.	-0.22717D 07
2	38662.	-0.21430D 07
3	-31443.	-0.18193D 07
4	-46162.	-0.14334D 07
5	-27598.	-0.11448D 07
6	-7468.4	-0.10173D 07
7	-5081.3	-0.99940D 06
8	-5005.4	-0.10045D 07
9	-5152.0	-0.10006D 07
10	-4923.6	-0.99825D 06
11	-5237.5	-0.10017D 07
12	-3399.1	-0.10010D 07
13	-7444.2	-0.99792D 06
14	-3635.2	-0.99765D 06
15	-5265.8	-0.10009D 07
16	-4963.8	-0.99989D 06
17	-4983.9	-0.99806D 06

NP	NODAL POINT DISPLACEMENTS
1	0.13157D-02
2	0.11784D-02
3	0.86677D-03
4	0.62037D-03
5	0.51822D-03
6	0.50099D-03
7	0.50035D-03
8	0.49977D-03
9	0.49981D-03
10	0.49984D-03
11	0.50032D-03
12	0.50019D-03
13	0.49695D-03
14	0.49939D-03
15	0.49947D-03
16	0.49921D-03
17	0.49944D-03

R; T=10.40/12.73 10.28.52

Fig. 5. Output Example (cont.)

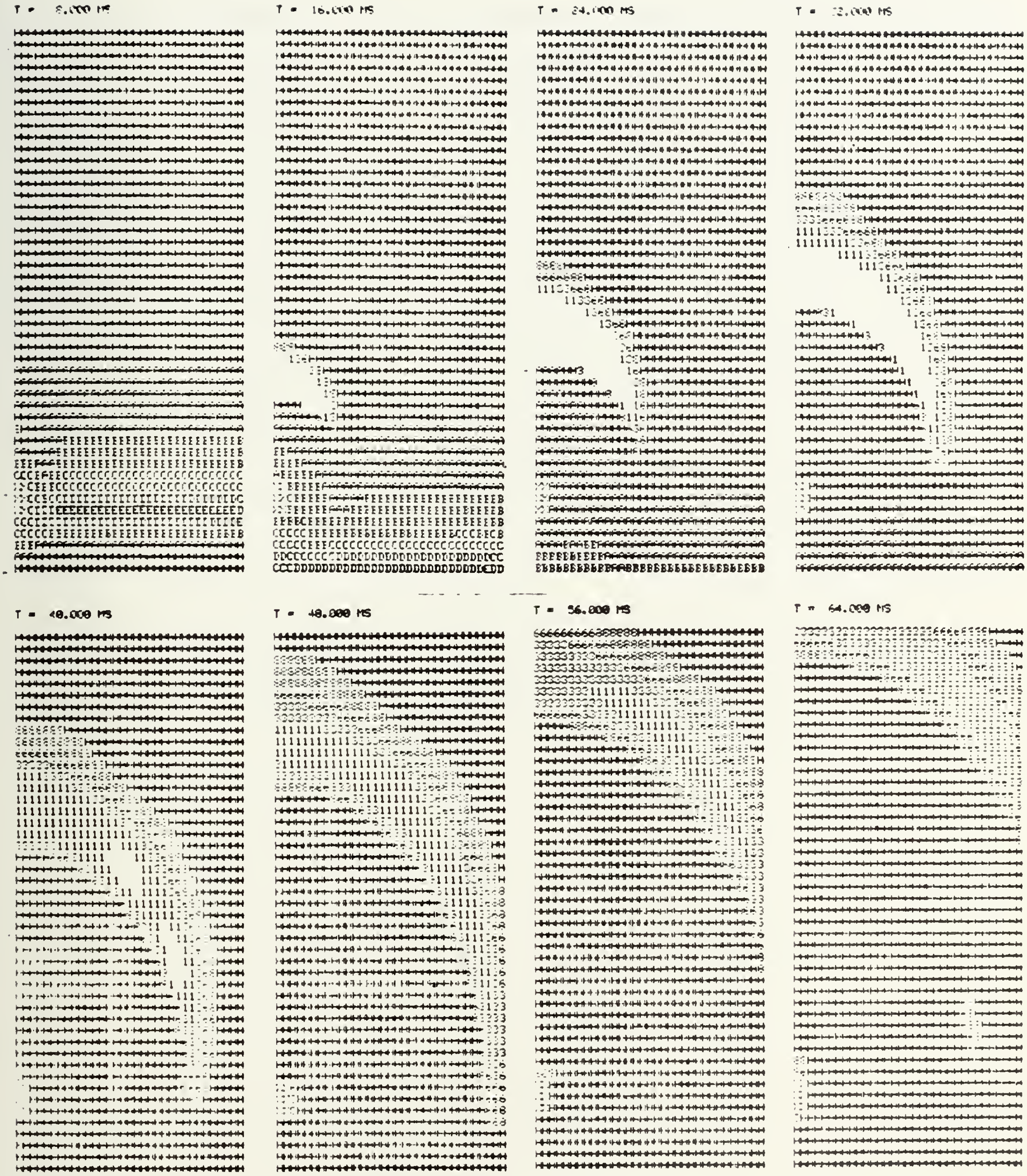

Fig. 6. Cavitation Example

Symbol	Pressure Range (m pa)
X	Structure
blank	Cavitated
1	0 - .04
3	.04 - .09
6	.09 - .14
8	.14 - .18
H	.18 - .43
A	.43 - .77
B	.77 - 1.10
C	1.10 - 1.43
D	1.43 - 1.77
E	1.77 - 2.10
F	over 2.10

Figure 7. Pressure Code

V. CONCLUSIONS AND RECOMMENDATIONS

The comparisons made between the program results where convergence of the solution has been obtained to results obtained by other methods, show that the model satisfactorily predicts the dynamic response of a ring to external pressures. The ring model cannot predict exactly the behavior of a real structure such as a submarine hull. However, by a suitable choice of ring parameters the response of the ring structure will provide a good first approximation to the response of a real structure.

A useful improvement to the program would be to include a section which would automatically pick out maximum values of bending moments and axial forces in the ring as well as when and where they occur. This would allow any desired time intervals between data printout to be used without missing peak responses.

APPENDIX

PROGRAM LISTING

```
C       XP-PRESSURES AT NODAL POINTS AT THE INSTANT OF TIME BEING EXC.
C       CCSINE-MATRIX OF TERMS, COSINE (NIPI/NNEL)
C       AN-FOURIER COSINE COEFFICIENTS ASS OCIATED WITH RADIAL DISPL.
C       BN-FOURIER SINE COEFFICIENT ASSO. WITH TANGENTIAL DISPL.
C       ANDOT-1ST TIME DERIVATIVE OF AN
C       ANDDT-SECOND TIME DERIVATIVE OF AN
C       BNDOT-1ST TIME DERIVATIVE OF BN
C       BNDDT-2ND TIME DERIVATIVE OF BN
C       NNEL-NUMBER OF ELEMENTS
C       NNP-NUMBER OF NODAL POINTS
C       XK1N-STIFFNESS COEFFICIENTS FOR FLEXURAL MODE
C       XM1N-MASS CODFFICIENTS FOR FLEXURAL MODE
C       XKA1N-STIFFNESS COEFF. ASSO. WITH RADIAL DISPL. USED IN
C      *CALCULATING ANDDT
C       XKB1N-STIFFNESS COEFF. ASSO. WITH TANGENTIAL DISPL. USED IN
C      *CALCULATING ANDDT
C       XMA1N-MASS COEFF. ASSO. WITH RADIAL DISPLACEMENT
C       XKA2N-STIFFNESS COEFF. ASSO. WITH RADIAL DISPL. USED IN
C      *CALCULATING BNDDT
C       XKB2N-STIFFNESS COEFF. ASSO. WITH TANGENTIAL DISPL. USED IN
C      *CALCULATING BNDDT
C       NNPA1N-MAXIMUM NUMBER OF MODES FOR WHICH AN AND BN ARE SOLVED
C      *FOR SIMULTANEOUSLY
C       NNPA2N-MAXIMUM NO. OF MODES INCLUDED IN CALCULATIONS
C       K,L,LLL,LLLL-COUNTERS
C       HT-TIME INCREMENT
C       RHO-DENSITY OF RING MATERIAL
C       AA-CROSS SECTIONAL AREA
C       RI-RADIUS OF GYRATION
C       R-RADIUS OF RING
C       E-MATERIAL MODULUS OF ELASTICITY
C       MM-NUMBER OF LOOPS DESIRED BETWEEN PRINTOUTS
C       ZN-NORMAL FORCE IN RING
C       ZM-BENDING MOMENT
C       W-RADIAL DISPLACEMENT
C       PH-HYDROSTATIC PRESSURE
C       ZFI-PI
C       THETA-ANGLE BETWEEN NORMAL TO SHOCK FRONT AND LOCATION ON RING


        SUBROUTINE IINPUT


        IMPLICIT REAL*8(A-H,O-Z)
        COMMON/OUT/K(20)
        CCMMON/SINT/NNEL,NNP,MM,NN,NNPA1N,NNPA2N,L,LLL
```

```
      COMMON/REAL/HH,AA,E,R,RI,RHO,GC,TI
      COMMON/VECTS/XP(50),COSINE(50,50),ANDDT(50),BN(50)
     *,BNDDT(50),ANDOT(50),BNDOT(50),XKA1N(50),XMA1N(50),AN(50)
     *,XKA2N(50),XKB1N(50),XKB2N(50),CN(50),XM1N(50),XK1N(50)
      COMMON/IPASS/DT,A,PH,N
      COMMON/SPASS/PASS(50)

C     READ NEEDED CONSTANTS

      ZPI=4.D0*DATAN(1.D0)
      NNP=4*N+1
      NNEL=NNP-1
      HH=DT
      R=A
      L=0
      READ(5,26)MM
      READ(5,27)AA,E,RI,RHO
26    FORMAT(6I5)
27    FORMAT(7G10.3)
      EXTN=2*ZPI*R/((5*DT)*(E/RHO)**.5)
      FLEXN=(EXTN*R/RI)**.5
      NNPA1N=EXTN
      NNPA2N=FLEXN
      IF(NNP.LT.NNPA1N)NNPA1N=NNP
32    IF(NNP.LT.NNPA2N) NNPA2N=NNP
      RETURN
      END


      SUBROUTINE COEFFI


      IMPLICIT REAL*8(A-H,O-Z)
      COMMON/SINT/NNEL,NNP,MM,NN,NNPA1N,NNPA2N,L,LLL
      COMMON/REAL/HH,AA,E,R,RI,RHO,GC,TI
      COMMON/VECTS/XP(50),COSINE(50,50),ANDDT(50),BN(50)
     *,BNDDT(50),ANDOT(50),BNDOT(50),XKA1N(50),XMA1N(50),AN(50)
     *,XKA2N(50),XKB1N(50),XKB2N(50),CN(50),XM1N(50),XK1N(50)
      COMMON/IPASS/DT,A,PH,N

      RIR=RI/R
      EAORS=E*AA/(R*R)
      RA=RHO*AA
      EORHRS=E/(RHO*R**2)
      Z=RIR**2
      ZPI=4.D0*DATAN(1.D0)

C     FORM FOURIER COEFFICIENTS FOR PRESSURE REPRESENTATION AND
```

```
C       FORM MASS AND STIFFNESS COEFFICIENTS

        DC 500  I=1,NNP
        XI=I
        DO 505  J=1,NNP
        XJ=J
        XNEL=NNEL
        THETA=(XI-1.DO)*(XJ-1.DO)*ZPI/XNEL
        COSINE(I,J)=DCOS(THETA)
505     CONTINUE
        XI=XI-1.DO
        XMAIN(I)=RA*(1.DO+Z*XI**2)
        XKAIN(I)=EAORS*(Z*(XI**2-1.DO)**2+1.DO)
        XKBIN(I)=EACRS*XI
        XKA2N(I)=EORHRS*XI
        XKB2N(I)=EORHRS*XI**2
        IF(I.EQ.1)GC TO 582
        XMIN(I)=RA*((XI**2+1.DO)/XI**2+Z*XI**2)
582     XKIN(I)=EAORS*(RIR**2*(XI**2-1.DO)**2)
500     CONTINUE
        CALL PRINT2(14)

C       SET COEFFICIENTS = 0 INITALLY

        PH=PH/XKAIN(1)
        DO 526  I=1,NNP
        AN(I)=0.DO
        ANDOT(I)=0.CO
        BNDOT(I)=0.DO
526     EN(I)=0.DO
        AN(1)=PH
        LLL=1
        TI=0.DO
        L=1
        RETURN
        END

        SUBROUTINE TIMSTP

        IMPLICIT REAL*8(A-H,O-Z)
        COMMON/SINT/NNEL,NNP,MM,NN,NNPAIN,NNPA2N,L,LLL
        COMMON/REAL/HH,AA,E,R,RI,RHO,GC,TI

        CALL PINPUT
        CALL CNS
        TI=LLL*HH
        CALL PREDIC
        CALL MOMFOR
```

```
      CALL DISPLA
      L=L+1
      LLL=LLL+1
      RETURN
76    STOP
      END


      SUBROUTINE PINPUT


      IMPLICIT REAL*8(A-H,O-Z)
      COMMON/SINT/NNEL,NNP,MM,NN,NNPA1N,NNPA2N,L,LLL
      COMMON/REAL/HH,AA,E,R,RI,RHO,GC,TI
      COMMON/VECTS/XP(50),COSINE(50,50),ANDDT(50),BN(50)
     *,BNDDT(50),ANDOT(50),BNDOT(50),XKA1N(50),XMA1N(50),AN(50)
     *,XKA2N(50),XKB1N(50),XKB2N(50),CN(50),XM1N(50),XK1N(50)
      COMMON/SPASS/PASS(50)
5     FORMAT(6G10.2)
      DO 6 I=1,NNP
6     XP(I)=PASS(I)
      XP(1)=XP(1)/2.D0
      XP(NNP)=XP(NNP)/2.D0
      CALL PRINT2(15)
      RETURN
      END


      SUBROUTINE CNS


      IMPLICIT REAL*8(A-H,O-Z)
      COMMON/SINT/NNEL,NNP,MM,NN,NNPA1N,NNPA2N,L,LLL
      COMMON/REAL/HH,AA,E,R,RI,RHO,GC,TI
      COMMON/VECTS/XP(50),COSINE(50,50),ANDDT(50),BN(50)
     *,BNDDT(50),ANDOT(50),BNDOT(50),XKA1N(50),XMA1N(50),AN(50)
     *,XKA2N(50),XKB1N(50),XKB2N(50),CN(50),XM1N(50),XK1N(50)

C       SOLVE FOR CN'S

      DO 60 I=1,NNP
      C=0.D0
      DO 65 J=1,NNP
      C=XP(J)*COSINE(I,J)+C
65    CONTINUE
      XNEL=NNEL
      CN(I)=(2.D0/XNEL)*C
      IF(I.EQ.1)CN(I)=CN(I)/2.D0
```

```
      IF(I.EQ.NNP)CN(I)=CN(I)/2.D0
60    CONTINUE
      RETURN
       END


      SLBROUTINE PREDIC


      IMPLICIT REAL*8(A-H,O-Z)
      CCMMON/SINT/NNEL,NNP,MM,NN,NNPA1N,NNPA2N,L,LLL
      COMMON/REAL/HH,AA,E,R,RI,RHO,GC,TI
      COMMON/VECTS/XP(50),COSINE(50,50),ANDDT(50),BN(50)
     *,BNDDT(50),ANDOT(50),BNDOT(50),XKA1N(50),XMA1N(50),AN(50)
     *,XKA2N(50),XKB1N(50),XKB2N(50),CN(50),XMIN(50),XK1N(50)

C     CENTRAL DIFFERENCE INTEGRATION OF D.E. TO PREDICT FUTURE A1N"S

      IF(LLL.NE.1)GO TO 541
      DC 542 I=1,NNP
      IF(I.GT.NNPA2N)GO TO 542
      IF(I.GT.NNPA1N)GO TO 543
      ANDDT(I)=(CN(I)-XKA1N(I)*AN(I)-XKB1N(I)*BN(I))/XMA1N(I)
      ANDOT(I)=-.5D0*ANDDT(I)*HH
      BNDDT(I)=-(XKA2N(I)*AN(I)+XKB2N(I)*BN(I))
      BNDOT(I)=-.5D0*BNDDT(I)*HH
      GO TO 542
543   ANDDT(I)=(CN(I)-AN(I)*XK1N(I))/XM1N(I)
      ANDOT(I)=-.5D0*ANDDT(I)*HH
542   CONTINUE
541   DO 540 I=1,NNP
      IF(I.GT.NNPA1N)GO TO 550
      XI=I
      ANDDT(I)=(CN(I)-XKA1N(I)*AN(I)-XKB1N(I)*BN(I))/XMA1N(I)
      ANDOT(I)=ANDOT(I)+ANDDT(I)*HH
      AN(I)=AN(I)+ANDOT(I)*HH
      BNDDT(I)=-(XKA2N(I)*AN(I)+XKB2N(I)*BN(I))
      BNDOT(I)=BNDOT(I)+BNDDT(I)*HH
      BN(I)=BN(I)+BNDOT(I)*HH
      GO TO 540
550   CONTINUE
      IF(I.GT.NNPA2N)GO TO 540
      ANDDT(I)=(CN(I)-AN(I)*XK1N(I))/XM1N(I)
      ANDOT(I)=ANDOT(I)+HH*ANDDT(I)
      AN(I)=AN(I)+HH*ANDOT(I)
      XI=I-1
      BN(I)=-AN(I)/XI
540   CONTINUE
```

```
      CALL PRINT2(17)
      RETURN
      ENC

      SUBROUTINE MOMFOR

      IMPLICIT REAL*8(A-H,O-Z)
      COMMON/DIS/W(50)
      COMMON/SINT/NNEL,NNP,MM,NN,NNPA1N,NNPA2N,L,LLL,LLLL,J
      COMMON/REAL/HH,AA,E,R,RI,RHO,GC,TI,ZN,ZM
      COMMON/VECTS/XP(50),COSINE(50,50),ANDDT(50),BN(50)
     *,BNDDT(50),ANDOT(50),BNDOT(50),XKA1N(50),XMA1N(50),AN(50)
     *,XKA2N(50),XKB1N(50),XKB2N(50),CN(50),XMIN(50),XK1N(50)
C     CALCULATE BENDING MOMEMTS AND AXIAL FORCE

      ZPI=4.DC*DATAN(1.DO)
      Z=(RI/R)**2
      LLLL=1
      C=-E*AA*RI**2/R**2
      B=E*AA/R
      DO 601 J=1,NNP
      ZM=0.DO
      ZN=0.DO
      DO 602 I=1,NNP
      XI=I-1
      XJ=J-1
      ZM=C*(1-XI**2)*AN(I)*DCOS(XI*XJ*ZPI/NNEL)+ZM
602   ZN=-B*(AN(I)*(1+Z*(1-XI**2))+XI*BN(I))*DCOS(XI*XJ*ZPI/NNEL)+ZN
601   CALL PRINT2(16)
      LLLL=1
      RETURN
      END

      SUBROUTINE DISPLA

      IMPLICIT REAL*8(A-H,O-Z)
      COMMON/DIS/W(50)
      COMMON/SINT/NNEL,NNP,MM,NN,NNPA1N,NNPA2N,L,LLL
      COMMON/REAL/HH,AA,E,R,RI,RHO,GC,TI
      COMMON/VECTS/XP(50),COSINE(50,50),ANDDT(50),BN(50)
     *,BNDDT(50),ANDOT(50),BNDOT(50),XKA1N(50),XMA1N(50),AN(50)
     *,XKA2N(50),XKB1N(50),XKB2N(50),CN(50),XMIN(50),XK1N(50)
      COMMON/SPASS/PASS(50)
```

```
C       FIND RADIAL DISPLACEMENT

        DO 570 I=1,NNP
        WT=0.DO
        DO 575 J=1,NNP
        V=AN(J)*COSINE(I,J)
        WT=WT+V
575     CONTINUE
        W(I)=WT
        PASS(I)=W(I)
570     CONTINUE
        CALL PRINT2(18)
        RETURN
        END


        SUBROUTINE PRINT2(LL)


        IMPLICIT REAL*8(A-H,O-Z)
        COMMON/DIS/W(50)
        COMMON/OUT/K(20)
        COMMON/SINT/NNEL,NNP,MM,NN,NNPA1N,NNPA2N,L,LLL,LLLL,J
        COMMON/REAL/HH,AA,E,R,RI,RHO,GC,TI,ZN,ZM
        COMMON/VECTS/XP(50),COSINE(50,50),ANDDT(50),BN(50)
       *,BNDDT(50),ANDOT(50),BNDOT(50),XKA1N(50),XMA1N(50),AN(50)
       *,XKA2N(50),XKB1N(50),XKB2N(50),CN(50),XM1N(50),XK1N(50)

        IF(L.EQ.0)GO TO 91
        IF(L.EQ.MM)GO TO 91
        GO TO 1
91      IF(K(LL).EQ.1) GO TO 1
        GO TO (1,1,1,1,1,1,1,1,1,1,1,1,1,14,15,16,17,18),LL
1       RETURN

C       PRINT INPUT DATA & MASS AND STIFFNESS COEFFICIENTS


14      WRITE(6,978)
978     FORMAT(/3X,'STRUK5',/)
        WRITE(6,85)
85      FORMAT(/3X,'NNEL   NNP   MM NNPA1N NNPA2N',/)
27      FORMAT(10X,5G10.3)
        WRITE(6,26)NNEL,NNP,MM,NNPA1N,NNPA2N
        WRITE(6,90)
90      FORMAT(/,13X,'A',9X,'E',9X,'R',9X,'RI',7X,'RHC',/)
        WRITE(6,27)AA,E,R,RI,RHO
```

```
26      FORMAT(6I5)
        WRITE(6,1010)
1010    FORMAT(/,6X,'I',8X,'XKA1N',8X,'XKA2N',8X,'XMA1N',8X,'XKB1N')
        WRITE(6,1015)(I,XKA1N(I),XKA2N(I),XMA1N(I),XKB1N(I),
       *I=1,NNP)
1015    FORMAT(I8,2X,4G13.5)
        RETURN


C       PRINT INPUT PRESSURE


15      WRITE(6,75)
        XP(1)=XP(1)*2.D0
        XP(NNP)=XP(NNP)*2.D0
75      FCRMAT(/,3X,'NODAL POINT PRESSURES',/)
        WRITE(6,5)(XP(I),I=1,NNP)
        XP(1)=XP(1)/2.D0
        XF(NNP)=XP(NNP)/2.D0
5       FORMAT(6G10.2)
        RETURN


C       PRINT BENDING MOMENTS & AXIAL FORCES


16      IF(LLLL.NE.1)GO TO 606
        LLLL=LLLL+1
        WRITE(6,604)
604     FORMAT(/,'          NP                    MCMENT                    FORCE',/)
606     WRITE(6,603)J,ZM,ZN
603     FCRMAT(3X,I5,8X,G15.5,8X,G15.5)
        RETURN


C       PRINT TIME, AN,BN, & CN


17      WRITE(6,70) TI
70      FORMAT(/,3X,'TIME =',3PF8.3,' MS')
        WRITE(6,1020)
1020    FORMAT(/,2X,'        BN                    AN                    CN')
        WRITE(6,1000)(BN(I),AN(I),CN(I),I=1,NNP)
1000    FORMAT(3G15.5)
        RETURN


C       PRINT NODAL POINT DISPLACEMENTS
```

```
18    WRITE(6,80)                                              STR03850
      WRITE(6,35)(I,W(I),I=1,NNP)                              STR03860
35    FORMAT(I5,12X,G15.5)                                     STR03870
80    FORMAT(/,'    NP    NODAL POINT DISPLACEMENTS',/)        STR03880
      L=0                                                      STR03890
      RETURN                                                   STR03900
      END                                                      STR03910
                                                               STR03920
                                                               STR03930
```

LIST OF REFERENCES

1. Newton, R.E., "Effects of Cavitation on Underwater Shock Loading - Part 1," NPS-69-78-013, Naval Postgraduate School, Monterey, CA, July 1978.

2. Newton, R.E., "Effects of Cavitation on Underwater Shock Loading - Plane Problem, Part I," NPS-69-79-007PR, Naval Postgraduate School, Monterey, CA, July 1979.

3. Timoshenko, S., Strength of Materials, Part I. New York: D. Van Nostrand Company, Inc., 1955.

4. Timoshenko, S., Theory of Plates and Shells. New York: McGraw-Hill Book Company, Inc., 1959.

5. Newton, R.E., "Some Matrix Applications to Vibration Problems," Class Notes, Naval Postgraduate School, Jan. 1975.

6. Roark, R.J., and Young, W.C., Formulas For Stress And Strain, New York: McGraw-Hill Book Company, 1975.

INITIAL DISTRIBUTION LIST

		No. Copies
1.	Defense Documentation Center Cameron Station Alexandria, Virginia 22314	2
2.	Library, Code 0142 Naval Postgraduate School Monterey, California 93940	2
3.	Department Chairman, Code 69 Department of Mechanical Engineering Naval Postgraduate School Monterey, California 93940	2
4.	Professor. R. E. Newton, Code 69Ne Department of Mechanical Engineering Naval Postgraduate School Monterey, California 93940	5
5.	Jack T. Waller Jr., Code 3354 FUZE Department Naval Weapons Center China Lake, CAlifornia 93555	1
6.	Dr. Eugene Sevin SPSS Defense Nuclear Agency Washington, D. C. 20305	1
7.	Dr. Gordon C. Everstine, Code 1844 David W. Taylor Naval Ship Research and Development Center Bethesda, Maryland 20084	1
8.	Commander Naval Weapons Center China Lake, California 93555 ATTN: Code 533 (Tech Lib)	1
9.	Dr. Melvin L. Baron Weidlinger Associates 110 East 59th Street New York, New York 10022	1
10.	Dr. Thomas L. Geers Dept. 52-33/Bldg. 205 Lockheed Palo Alto Research Laboratory 3251 Hanover Street Palo Alto, California 94304	1

Thesis
W222715 Waller 187104
c.1
Dynamic structural
model of a submerged
ring.